FINITE ELEMENT ANALYSIS OF CONTRIBUTION OF ADHESION AND HYSTERESIS TO SHOE-FLOOR FRICTION

by

Seyed Reza Mirhassani Moghaddam

A Thesis Submitted in

Partial Fulfillment of the

Requirements for the Degree of

Master of Science

in Engineering

at

University of Wisconsin-Milwaukee

December 2013

ABSTRACT

FINITE ELEMENT ANALYSIS OF CONTRIBUTION OF ADHESION AND HYSTERESIS TO SHOE-FLOOR FRICTION

by

Seyed Reza Mirhassani Moghaddam

The University of Wisconsin-Milwaukee, 2013
Under the Supervision of Professor Kurt E. Beschorner

Slips and falls are one of the leading causes of occupational accidents. Understanding the important factors that affect shoe-floor friction is vital for identifying unsafe surfaces and designing better footwear and flooring. While the shoe-floor coefficient of friction is known to be dependent on several factors including shoe and floor roughness, shoe speed, shoe material, and normal load, the mechanisms that cause these effects are not very well understood. The objective of this thesis is to develop a finite element model that simulates the microscopic asperity interaction between shoe and floor surfaces and apply it to quantify the effect of shoe material, topography, loading and sliding speed on shoe-floor adhesion and hysteresis friction.

Recent studies have concluded that boundary lubrication is highly pertinent to slipping and that adhesion and hysteresis are the main friction components in boundary lubrication. To have a better knowledge about the mechanisms governing the boundary lubrication friction at the microscopic asperity interaction level, a three dimensional computational model of two rough surfaces is developed which calculates the friction force due to hysteresis and real area of contact (which is proportional to adhesion

friction). The computer model includes two rough surfaces of rubber and rigid material. A viscoelastic material model based on parameters calculated from experiments is used to simulate the shoe material. In addition, surface to surface contact algorithm is used for simulating the interaction of the two rough surfaces. The results show that microscopic shoe and floor roughness, followed by material properties, shoe sliding speed, and normal loading affect hysteresis and adhesion coefficient of friction. The model provides an improved insight about the mechanisms that cause changes in adhesion and hysteresis when altering shoe and floor roughness, sliding speed, shoe material and normal loading and it can be useful in development of slip resistant shoes and floorings.

TABLE OF CONTENTS

LIST OF FIGURES

LIST OF TABLES

LIST OF NOMENCLATURE

COF- Coefficient of friction

R_z - Average peak-to-valley distance of surface profile

G_0 - Short time shear modulus,

G_∞ - Long time shear modulus,

β - Decay constant

$G(t)$ - Variation of shear modulus with respect to time

K_0 - The slope of the loading portion of the relaxation curve

$F_{0.02}$ - Force in two percent of total thickness of elastomers

F_0 - Peak force applied to elastomer samples

K_∞ -The slope of the straight line connecting the force in 2 percent of total thickness and the asymptotic force

F_∞ - Asymptotic force applied to elastomers

T - Average thickness of shoe samples

E_0 - Short time compressive modulus

E_∞ - Long time compressive modulus

A - Average surface area of elastomers

G - Shear modulus

E - Compressive modulus

v - Poisson's ratio

K - Bulk modulus

$COF_{Hysteresis}$ - Coefficient of friction due to hysteresis

$COF_{Adhesion}$ - Coefficient of friction due to adhesion

$F_{Adhesion}$ –Frictional force due to adhesion

F_{Normal} – Loading force normal to the surface

ACKNOWLEDGEMENTS

I would like to thank my graduate advisor, Dr. Kurt Beschorner, for providing me with the opportunity to research in this field which make up this work. While performing this research, his guidance and support, while still allowing me the freedom to learn first-hand, proved to be instrumental in the advancement of my work. His high standards and commitment to research set a strong example for me in my time in the lab, and provided me with the motivation necessary to perform the required tasks. I also want to thank Dr. Pradeep Menezes for his valuable time and continuous guidance throughout the course of this research. I would not have been able to complete this work without his support. I also want to thank Dr. Michael Nosonovsky for accepting my invitation to serve as committee member and help in improving the quality of this work. Finally, I am grateful to my parents Hojjat and Narges for boosting my morale and providing me the opportunity to achieve my desired goals throughout my life. I also thank all my friends at University of Wisconsin-Milwaukee.

1.Introduction

1.1 . Significance of Slips, Trips and Falls

Slip, trip and fall accidents are a major occupational health and economic burden. The National Floor Safety Institute has stated that slips and falls are the primary cause of workers' compensation claims [1]. According to Liberty Mutual Workplace Safety Index, fall accidents had the highest percentage of cost growth trends among the most disabling workplace injuries between 1998 and 2010 [2]. Slips, trips, and falls are also responsible for 15% of all accidental deaths [3] and 15% of total fatal occupational injuries in 2012 [4]. Out of this 15%, 80 % of falls can be categorized as falls to lower level, 13 % of falls happened on the same level and 7% happened from a collapsing structure or equipment (Figure 1). For 2012, the Bureau of Labor Statistics reported a total number of 299,090 slips, trips and falls in the workplace, which account for roughly 25% of non-fatal occupational injuries. Falls on the same level, falls to lower level and slips and trips without fall, contributed to 15%, 5% and 5% of non fatal occupational injuries and required a median of 10 , 19 , and 10 days away from work to recover respectively [5]. The incident rate for non-fatal occupational injuries for fall to lower level, fall on same level, and slips or trips without fall were 5.6, 18.2 and 4.8 per 10,000 full time workers respectively [5]. Falls on the same level were the second most disabling and costly occupational accident costing $8.61 billion and accounting for 16.9 % of the total injury burden in 2010 while falls to lower level accounted for 10% disabling injuries resulting in a $5.12 billion expense in that year [2]. Therefore, preventing slips and falls is of great importance.

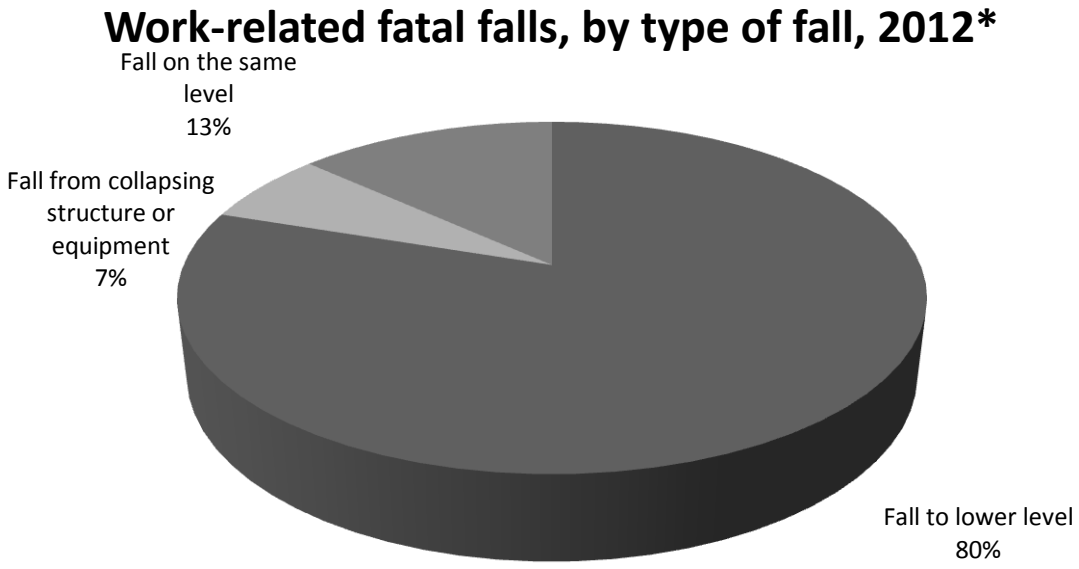

Figure 1. Work related fatal falls, by type of fall occurred in 2012. * Preliminary data for 2012 (Adapted from BLS, 2012)

1.2 . Shoe-Floor Friction

Slipping is the main initiating event that results in a fall [6]. The friction between the shoe and floor is regarded as the primary contributing factor to slipping accidents. Investigating the friction or coefficient of friction (COF) between shoe and floor is a method for estimating slipperiness. Research has shown that probability of slips and falls increases as the available coefficient of friction becomes less than the required coefficient of friction [7,11]. The required coefficient of friction is the ratio of shear force and normal force that is necessary to maintain normal human gait. The mean required coefficient of friction is reported to be between from 0.17 to 0.22 for normal walking on level surfaces [7-10], so in general the available coefficient friction must be higher than this value in order to prevent slipping [12].

There are multiple factors that affect the available coefficient of friction between shoe and flooring. These factors can be roughly grouped either as person-specific or as environmental factors [13]. Person-specific factors include choice of footwear (i.e. material and tread pattern) [14-18] and biomechanical factors, which include gait style (i.e. cadence, step length) [13,18] and walking speed [19-21]. Environmental factors include flooring design (i.e. floor material [17,22], floor roughness [18,23] and floor waviness [24]), existence of a fluid contaminant [17,19-21,25] and floor sloping [13]. The severity of a slip depends on both types of factors.

Shoe-floor interface friction is a very complicated tribological phenomenon. A broad and thorough understanding of the mechanisms behind this complex phenomenon will enable shoe and flooring manufacturers to design better shoe soles and floor surfaces to enhance the slip resistance capabilities and decrease slips. While the principles of tribology has been successfully applied to other fields of study such as artificial joints, bearings, gears and tires, in improving designs and reducing friction and wear, there is a paucity of research focusing on shoe-floor friction.

Earlier studies has identified the main components of dry friction in elastomers as adhesion, hysteresis and tearing [26-28] but the main focus of these papers is on tire friction that might be working in conditions dissimilar to shoe-floor system. Adhesion and hysteresis are relevant to the friction in dry-shoe-floor interface and lubricated-shoe-floor interface. Adhesion occurs when the two surfaces are pushed against each other and the asperities of the contacting surfaces create an adhesional bond [29]. This bond requires shear force to be broken. Contact area, which is dependent on the asperity geometry, roughness and elastic modulus; and surface energy, which is a function of the

two materials, are regarded as parameters affecting adhesion [27]. Hysteresis is due to energy loss during deformation of the softer shoe/rubber when the deformation energy throughout loading is larger than the recovery energy. In both adhesion and hysteresis phenomena, loss of energy occurs. In adhesion, this energy is dissipated in the contacting zone, while hysteresis causes the energy loss to take place in a depth inside the rubber at the vicinity of maximum shear stress [25].

In the presence of a contaminant, boundary lubrication [17,19] and hydrodynamic lubrication [9,20-21,25,28] are reported as the two different lubrication mechanisms pertinent to shoe-floor-contaminant friction [21]. In boundary lubrication, the fluid does not have a significant effect on hysteresis but affects the adhesion component [17]. Relative to other lubrication regimes, coefficient of friction is greatest in boundary lubrication [30]. Hydrodynamic effects (including the mixed, elasto-hydrodynamic and hydrodynamic lubrication parts of the Stribeck curve), cause an increase in the fluid pressure between shoe and floor and this fluid pressure increase results in a separation and reduction of contact between the surfaces [20,30]. This separation can cause the available friction to approach zero [31]. The available coefficient of friction should always be greater than the required coefficient of friction to decrease the chances of slip. Thus, slip-resistant designs that manipulate lubrication in a way that increases friction above these levels would prevent slipping incidents.

1.3 . Computational Modeling of Shoe-Floor Friction

Development of a computational model for shoe-floor friction would be beneficial to comprehend the friction mechanisms relevant to dry and contaminated surfaces. This model will provide the opportunity to independently understand the effects of different

factors including shoe/floor roughness, shoe/floor material properties, speed and contact pressure on different friction components (i.e. adhesion and hysteresis). The shoe-floor interaction can be modeled using a viscoelastic material against a hard surface since viscoelastic rubber polymers are typically used as shoe materials. Viscoelastic materials have the ability to distribute the pressure under the shoe in order to decrease forces at local points [32]. This viscoelastic properties also help in absorbing and dampening the shocks during the shoe impact on the floor [33]. During contact between an elastomeric material and a rough surface, adhesion and hysteresis are the primary friction mechanisms [26,27]. Finite element analysis using a viscoelastic material is capable of simulating the adhesion and hysteresis behavior of shoe materials and will increase our knowledge about the above-mentioned hysteresis and adhesion components of friction.

Computational models of the shoe-floor interaction have been implemented previously in order to quantify friction and determine how forces are transmitted to the foot. Recently, Cheung et al. provided a broad review of most of the finite element models developed so far with regard to shoe and footwear [34], however the aim of most of the research mentioned in the paper can be categorized either as increasing athletic performance of the shoes or decreasing the pressures applied to the foot during walking/running. From that perspective, they suggested the use of computer aided engineering software to create geometries of foot from medical images and then using finite element method for finding the stresses and identifying the vulnerable skeletal and soft tissues and the load transfer mechanism of shoe and foot. Similarly, Lewis et al, used a finite element model to evaluate the effect of choosing two different materials for shoe outsole on the stresses developed between shoe and foot [35]. A footwear and ground

finite element model was also developed to understand the deformation of soil mass between boots and soft soil in which five different models of different tread design were investigated [36]. This study, however, was only limited to outdoor soil surfaces and had little relevance to preventing slips indoors. There is no study that rigorously implements finite element method for investigating the components of shoe-floor friction either in microscopic or macroscopic level.

In other disciplines, experimental and finite element methods has been successfully used to model adhesion friction between rubber and a rigid surface. Pioneering work of Tabor concludes that during the contact of two rough surfaces, there is a difference between the real contact area and the geometrical contact area such that real contact area is always much less than the geometrical contact area [27]. In the real contact region, the two surfaces are loaded against each other and the peaks of the asperities of the two surfaces form adhesional bonds, and therefore shear force is required to break these bonds. Contact area, depends on the geometry of the contacting asperities, roughness, elastic modulus, vertical loading and surface energy of the two materials and is proportional to the adhesion friction force [27]. Increasing the contact pressure would increase the viscoelastic deformation and this increase would cause an increase in real contact area and can also increase the adhesion friction [37, 38]. Because contact area is proportional to adhesion, these studies provide insight into how these topographical, material and loading parameters influence adhesion friction. Moreover, finite element modeling has been demonstrated as a valid approach for estimating adhesion friction between a micro-scale rough rubber surface and metal surface asperities based on single asperity contact [39] and is validated using experimental results [37,38]. Applying similar

methods with multiple asperities to shoe and flooring may provide insight into shoe-floor-contaminant friction.

Hysteresis is reported to be related to the deformation energy loss of the softer rubber material occurring when the loading is higher than the recovery energy and results in the conversion of the strain energy to heat [40]. Since the asperities of the shoe will be exposed to the cyclic deformation during a slip on a rigid floor, hysteresis will be a contributor to the shoe-floor friction [40]. Typically, the ratio of shear to normal force is used as a measure of hysteresis friction in the case of the contact of rough surfaces. Several finite models have successfully quantified the hysteresis between elastomeric materials and rough surfaces; however the majority of these models are in the field of tire mechanics and rubber-metal contacts and several used simplifying assumptions [41-46]. In [46] the hysteretic friction at asperity level was studied by finite element technique although the topography of the surface was replaced by a combination of sine waves. Garcia et al.[41] used finite element to predict the hysteretic component of industrial rubber in contact and validated their model by comparing its results to a their simple experimental setup. Martinez et al. [42] modeled the contact of rubber-metal to predict wear in metal components yet this study implemented a linear elastic model for describing the behavior of rubber material in contact with metal surfaces. Another model uses profilometry to accurately model the roughness of rubber/metal in the finite element and it is validated through comparison with tribometer tests [43]. The aforementioned research proposes finite element simulation of the tribometer tests as a tool for calculating contact area, and predicting the coefficient of friction. Research done by Gabriel et al. [44] emphasizes the importance of surface geometry in rubber-rigid contact

and introduces a third component of friction related to geometrical effects. Work of Tokura [45] uses explicit finite element modeling to simulate the microscopic contact of rubber and road surface and provides valuable recommendations for modeling capabilities of this software with regard to rubber-rigid contacts. Previous research of our group [29] has successfully used LS-Dyna in modeling the microscopic contact of a rubber block and a rough surface and predicting the two different components of friction but the materials parameters used in that model were based on material parameters of a softball polyurethane [47], which are not materials currently being used for shoe sole. Applying FEA methods to shoe-floor microscopic interactions will increase our understanding of how different parameters including shoe roughness, floor roughness, material parameters and normal load will affect shoe-floor friction components.

1.4 .Overview/Specific Aims

Understanding the adhesion and hysteresis friction during the sliding motion of shoe sole over rough surface is of critical importance. This thesis applies robust computational methods to developing a shoe-floor microscopic computer model and analyzing effects of different shoe sole/floor roughnesses, speed, material hardness and load levels on adhesion and hysteresis friction. The modeling method is valid for dry and boundary lubrication friction since it does not include hydrodynamic effects.

A three-dimensional computational model of shoe-floor rough surface model will be developed. The following model is able to calculate the real contact area between the rough surfaces as an approach for quantifying adhesion friction. The model will also calculate shear force due to hysteresis, which is a measure of hysteresis coefficient of friction. The finite element analysis will be conducted with the loading conditions

relevant to a human slip, speeds pertinent to slipping, genuine viscoelastic shoe sole based on experimentally measured material properties and measured roughness parameters of shoe and floor samples to identify how these factors influence friction. This finite element model will present a useful tool for designing the shoe soles/ floors and decrease the chance of slip and fall accidents

Hence, the goals of this thesis are as follows:

1) Creating a three dimensional computer model of shoe sole and floor in microscopic level

2) Simulating the slipping movement of shoe sample on the floor

3) Applying the model to understand the effects of sliding speed, normal loading, shoe roughness, shoe material properties and floor roughness as well as their interactions contribution to shoe-floor friction.

4) Comparing the model results to experimental data in order to partially validate the model.

2. Methods

To identify the effect of shoe and floor roughness, shoe sliding speed, material properties of shoe and normal loading on hysteresis and adhesion friction, finite element analyses were conducted in LS-Dyna software. The steps required for the model development and simulation are creating the shoe and floor geometries with microscopic asperities, quantifying the viscoelastic material properties of shoe sample elastomers and implementing those into the model, applying appropriate boundary conditions for motion and contact force control and using non-linear contact formulations in the finite element software.

2.1. Roughnesses and Model Geometries

The materials simulated in the model were based on two shoe materials and three ceramic tiles with different roughness levels, which were physically measured to ensure that the model input were relevant to actual shoe and floor samples. The two shoe materials were neolite and rubber. Neolite had a Shore A hardness of 95 measured using a durometer and it is considered a standard raw material in shoe-floor friction research [48]. Rubber sample, cut from an ordinary type of work shoe, had a Shore A hardness value of 50. To ensure that the shoe roughness was relevant to actual shoe topography, rubber samples were cut from shoe sole materials and the roughness was measured. To ensure that floor roughness was relevant to actual flooring, ceramic tiles with three different roughness levels were considered. Roughness parameters were measured using a two-dimensional contact type stylus profilometer (Figure 2). Eight roughness measurements were collected on each of the shoe samples and floorings using a scan length of 12.5 mm and a cutoff length of 0.80 mm. The roughness was characterized with

the average peak-to-valley distance (R_z) averaged across the eight scans (Table 1) since this parameter has a strong positive correlation with coefficient of friction [49]. It should be mentioned that the neolite material while being harder, tended to have a lower roughness compared to the rubber shoe material, which is softer. In order to isolate the effects of roughness and material properties, simulations were conducted using both roughness levels and both shoe materials. The adhesion and hysteresis friction of the materials considered in this study have been characterized experimentally [50].

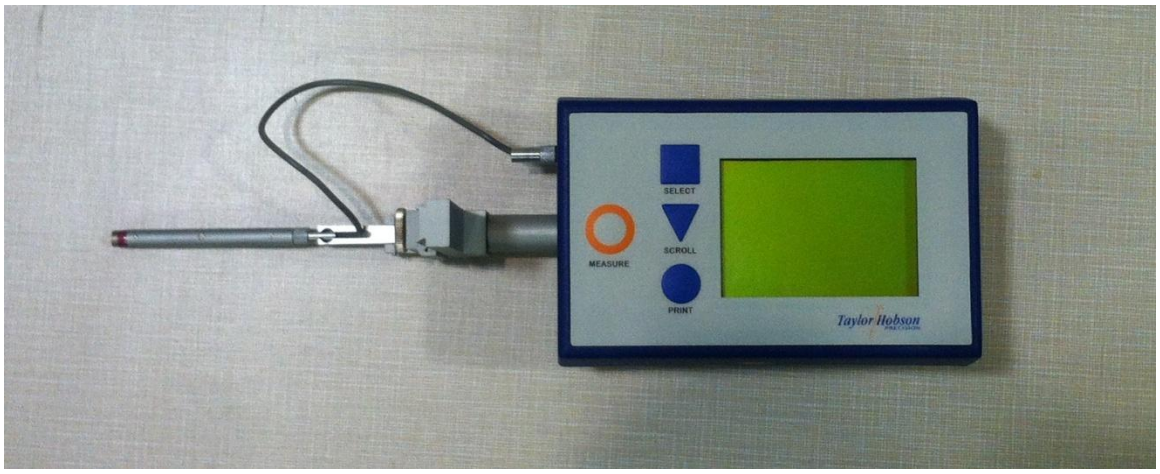

Figure 2. The profilometer device used for measuring roughness.

Table 1. Average peak to valley distance parameter (R_z) for shoe samples and floors

Shoe/Floor	Materials	Average peak to valley distance (R_z)
Shoe Samples	Neolite (Low)	12.1 µm
	Rubber (High)	35.1 µm
Floors	Low Roughness	16.6 µm
	Medium Roughness	24.3 µm
	High Roughness	35.1 µm

The three dimensional shoe sample models were created using solid brick elements in LS-Dyna. This type of elements is efficient and accurate in contact simulations and when exposed to severe deformations [51]. Surface nodes on the interface side of the shoe and floor samples were manually moved to create the roughness parameters shown in Table 1 (Figure 3) in a way that each peak/valley on the surfaces where half of the value of R_z above or below the baseline of the surface. The microscopic shoe sample models were 0.8 mm in length, 0.5 mm in width and 0.5 mm in height.

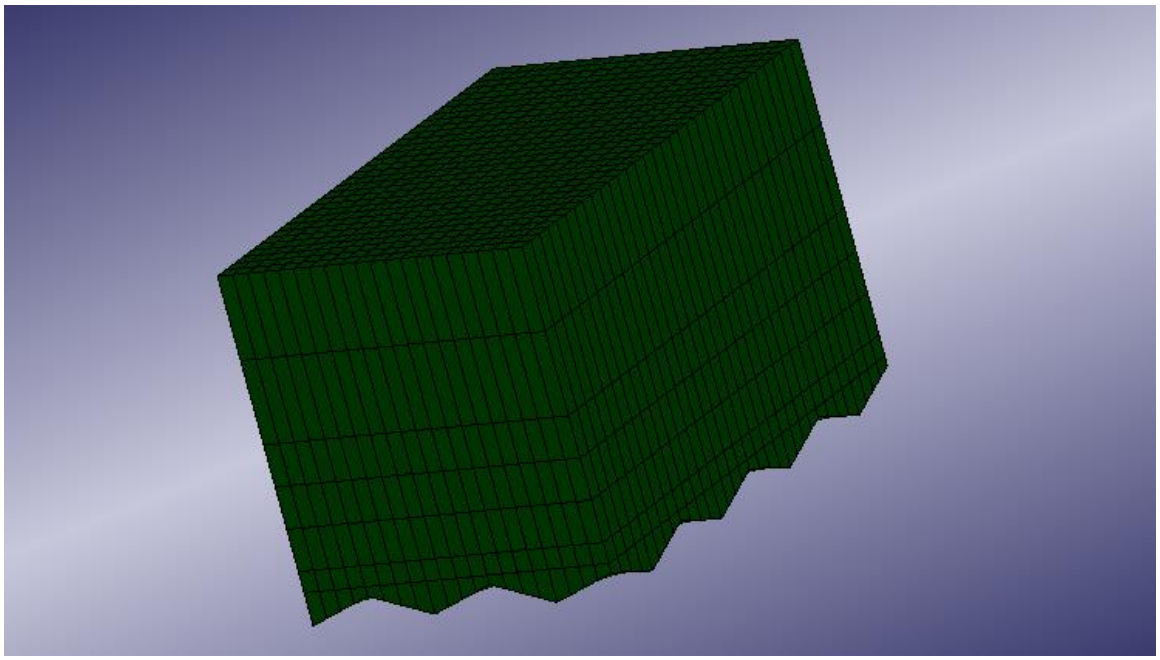

Figure 3. Shoe sample geometry model with asperities on the surface created in LS-Dyna.(High roughness)

Floor sample models were also created with microscopic asperities shown in Table 1 by using solid brick elements in LS-Dyna. The floor models were 2.125 mm in length, 1 mm in width and 0.135 mm in height. The model corresponding to the medium level roughness floor is shown in Figure 4. The complete geometrical picture of the aforementioned combination i.e. high roughness shoe- medium roughness floor is also

shown in Figure 5 including both of the shoe and floor. To determine if the accuracy was dependent on the mesh size, mesh refinement was performed and the results using mesh refinement were compared with results without mesh refinement. Because mesh refinement did not significantly impact the results, all simulations were performed without mesh refinement. Also, shoe samples were meshed such that in regions near the contact area a finer mesh was present and mesh size was increased with getting further from the contacting region (Figure 3). This was done in order to reduce the computation time.

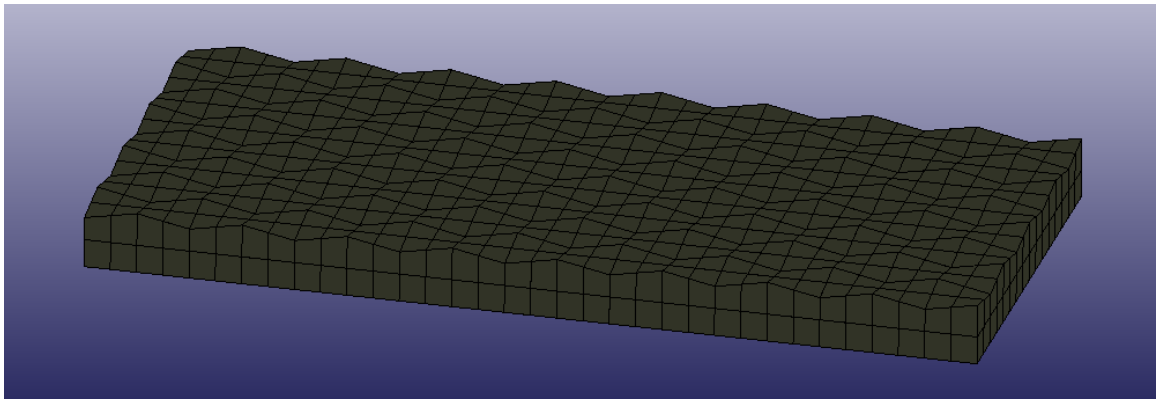

Figure 4. Floor geometrical model with asperities on the surface created in LS-Dyna. (Medium roughness)

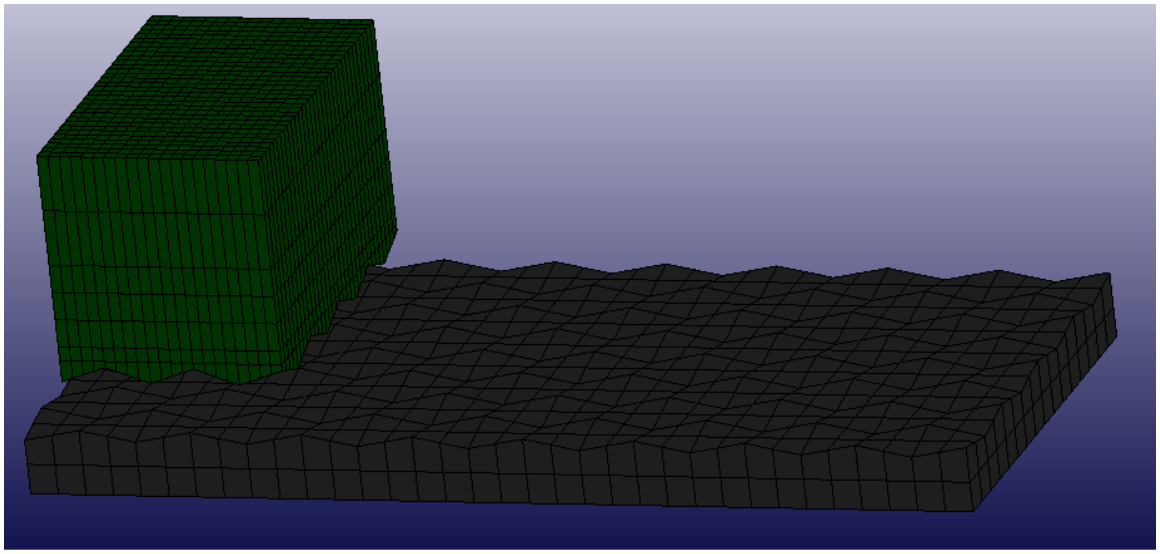

Figure 5. Shoe sample and floor with microscopic asperities created in LS-Dyna. (High shoe roughness and- medium floor roughness)

2.2. Material Properties

Material properties were measured from shoe samples and implemented into the model to ensure that the simulation results were relevant to actual shoes. When two materials with different hardness come into contact, most deformation occurs in the softer material so in the case of shoe-floor contact most of the deformation will take place in shoe material. Therefore, it was assumed that the floor sample material is un-deformable and it was modeled using a rigid material model. Initial models, which applied appropriate material properties for the flooring, revealed that results were very similar to simulations that used a rigid surface for the flooring. Shoe sample materials were implemented using a viscoelastic material model, which allows for hysteresis friction. This damping characteristic is particularly important in determining the hysteresis loss during the slipping. The viscoelastic material has a spring component to represent the elasticity of the shoe material and a damper representative of time varying properties.

The viscoelastic model describes shear stress relaxation of the viscoelastic material using a exponentially decaying function ([52] Equation 1).

$$G(t) = G_\infty + (G_0 - G_\infty)\mathrm{e}^{-\beta t} \quad \ldots (1)$$

where

G_0 : Short time shear modulus,

G_∞ : Long time shear modulus,

β : Decay constant and

G(t) : Variation of shear modulus with respect to time

LS-Dyna requires the user to input the density, short time shear modulus, long time shear modulus, bulk modulus and decay constant of the material. Density of the rubber was measured based on the volume and mass of the samples and was found to be 1100 kg/m^3 [53] for both materials. For determining the two shear moduli and bulk modulus, compressive stress relaxation experiment was conducted using MTS compression machine (MTS Systems Corporation, Eden Prairie, Minnesota, USA) (Figure 6.), according to the methods recommended for testing of elastomeric bearings [54]. Two rectangular blocks of shoe samples with approximately equal and uniform thickness were sandwiched between two steel plates. Figure 7 shows a schematic of the test setup used for the experiment. For each of the shoe materials the compression test was done three times. Average dimensions of the shoe sample blocks are also shown in Table 2. The testing method includes increasing the displacement applied to the shoe sample until a maximum level, here 10% of the sum of the two elastomer thicknesses, then applying this constant displacement level for a period of time, finally unloading the

samples and recording the force and displacement throughout the experiment. Once the force and displacements are recorded, the short and long time compressive moduli can be calculated using the methods provided in [54].

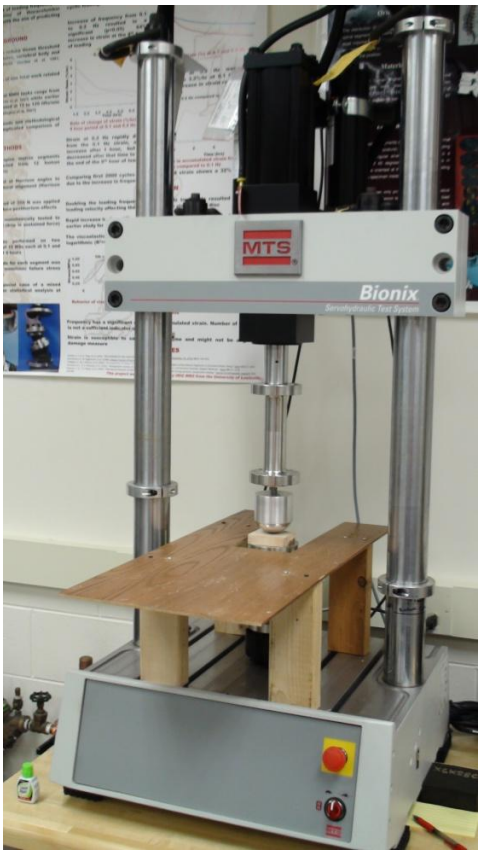

Figure 6. Compression testing machine used for the material parameters experiment

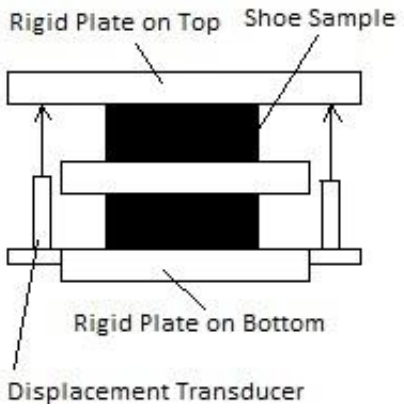

Figure 7. Schematic of test setup, (Adapted from [54]).

Table 2. Average thickness and area of the shoe samples

Material	Average Thickness (mm)	Average Area (mm^2)
Neolite	5.5	612
Rubber	6.1	552

Typical plots of displacement and force curves with respect to time are shown in Figures 8A and 8B, respectively. Both of the plots can be divided into three sections: loading where both displacement and force are increasing; stress-relaxation where displacement is constant and force decays; and unloading where displacement and force decrease back to 0. According to the methods in [54] K_0: the slope of the loading portion of the curve between compression of 2 percent of total thickness ($F_{0.02}$ in Figure 8B.) and the maximum force (F_0 in Figure 8B) can be used for calculating the short time compressive modulus (Equations 2 and 3). K_∞:The slope of the straight line connecting the force in 2 percent of total thickness ($F_{0.02}$ in Figure 9) and the asymptotic force (F_∞ in Figure 9) can also be used for calculating long time compressive modulus.(Equations 4 and 5).

$$K_0 = \frac{F_0 - F_{0.02}}{0.18T} \quad \ldots (2)$$

$$E_0 = K_0 \frac{2T}{A} \quad \ldots (3)$$

$$K_\infty = \frac{F_\infty - F_{0.02}}{0.18T} \quad \ldots (4)$$

$$E_\infty = K_\infty \frac{2T}{A} \quad \ldots (5)$$

where

T : Average thickness of shoe samples,

E_0: Short time compressive modulus,

E_∞: Long time compressive modulus,

A : Average surface area of elastomers

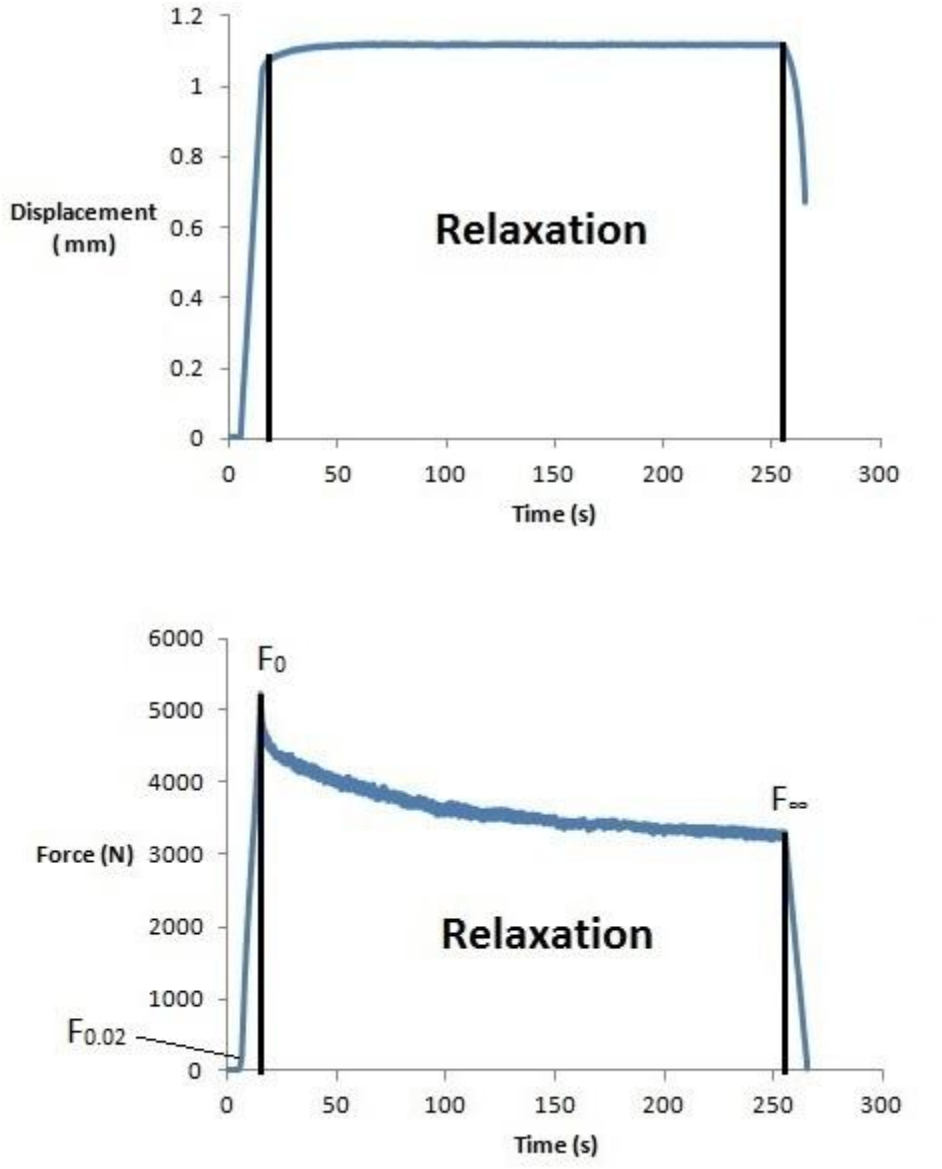

Figure 8. Plot of displacement (A) and force (B) versus time for one of neolite tests

After obtaining the values of short time and long time compressive moduli, rules of continuum mechanics are applied to find the short and long time shear moduli and bulk modulus. Rubber is usually categorized as a nearly incompressible material and is reported to have a Poisson's ratio of 0.49-0.499 [55]. These values for Poisson's ratio also have been used for finite element simulation of rubber using LS-Dyna [56]. In this thesis, all the simulations were conducted with a Poisson's ratio of 0.499 for the shoe sample.

Shear modulus, compressive modulus, Poisson's ratio and bulk modulus of a material are related and Equations 6 and 7 govern the relationship between these elastic constants [57]. With a value of 0.499 for Poisson's ratio, Equation 6 reduces to Equation 8 and can be used for determining shear moduli. After calculating short and long time shear modulus, bulk modulus can be calculated from Equation 7. Previous experimental studies have demonstrated that for viscoelastic materials, as Poisson's ratio approaches 0.5, bulk modulus can be assumed constant [58]. Thus, in all the simulations in this thesis, bulk modulus calculated using long time compressive modulus and long time shear modulus was used as the value of bulk modulus. In order to find aforementioned decay constant, an exponential curve fitting was done using a curve fitting toolbox (Matlab ®, Mathworks, USA) to find the coefficient of the exponential decay. An example of the output of this curve fitting process is shown in Figure 9. With applying all of these methods discussed in this section, the values of the parameters required for modeling viscoelastic behavior of shoe material were found and summarized in Table 3.

$$G = \frac{E}{2(1+\upsilon)} \quad \ldots (6)$$

$$K = \frac{EG}{3(3G-E)} \quad \ldots (7)$$

$$G \sim \frac{E}{3} \quad \ldots (8)$$

where

G : Shear modulus,

E : Compressive modulus,

υ : Poisson's ratio

K : Bulk modulus

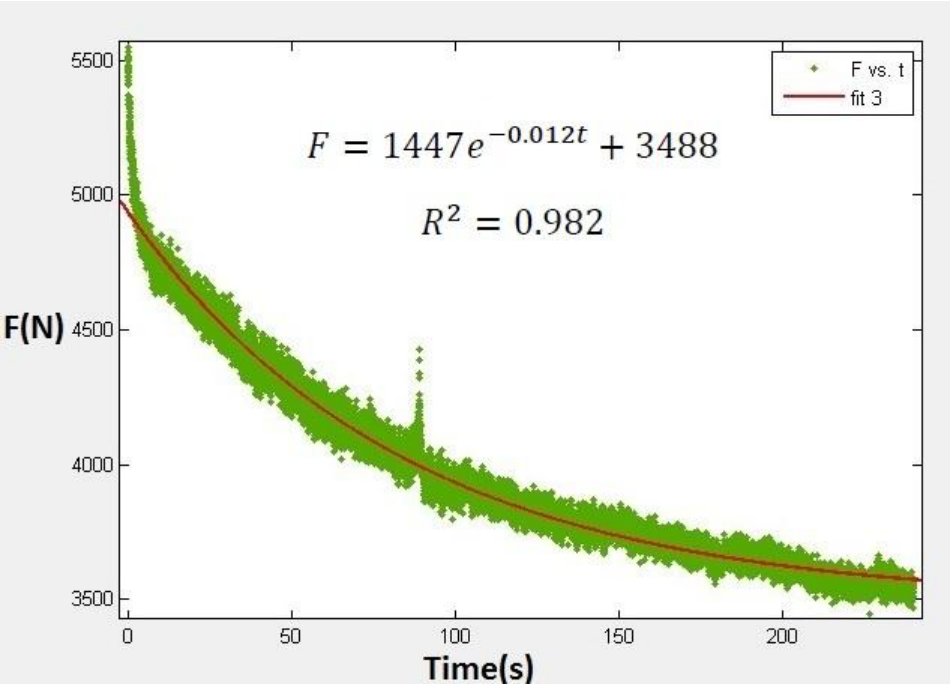

Figure 9. Curve fitting for neolite compression.

Table 3. Viscoelastic material parameters used for modeling neolite and rubber

Material	G_0 (MPa)	G_∞ (MPa)	K (MPa)	β (1/s)
Neolite	30.24	18.66	9324	0.013
Rubber	0.59	0.44	2180	0.025

2.3. Loadings and Boundary Conditions

Velocity boundary conditions were applied to the top surface of the shoe sample in order to move the shoe material relative to the floor material. During the first 0.001 seconds of the simulations, the shoe sample model was moved down and then a horizontal velocity was applied to the top surface until the termination of the simulation (i.e., the time that the shoe sample reached the end point of the floor sample). Previous research has recommended the requirements for biomechanically relevant, i.e. 'biofidelic' slip resistance testing and suggested a sliding speed at the shoe-floor interface between 0-1 m/s [25]. Therefore, Simulations were performed for 5 biofidelic sliding speeds, including 0.1, 0.25, 0.5, 0.75, and 1 m/s similar to [50] resulting in total simulation times of 0.0151, 0.007, 0.004, 0.003 and 0.0025 seconds respectively.

Compression of the shoe material was modified to achieve a range within the range of pressures that are considered biomechanically relevant. The biomechanically relevant range of contact pressure in shoe-floor interface is reported to be in the range of 100 to 1000 kPa [19]. The contact pressure was controlled using the downward displacement of the shoe meaning that, shoe sole was given three different boundary conditions such that it moved downward during the first 0.001 seconds of the simulation until it resulted in normal force level equivalent to contact pressures of 160, 260 and 360 kPa namely low, medium and high normal loads and then, it started moving horizontally. In all the simulations, the bottom surface of the floor was constrained from both translation and rotation.

2.4. Solution Algorithm and Contact Formulation

To identify the effect of shoe and floor roughness, sliding speed, shoe material properties and normal loading on hysteresis and adhesion friction, finite element analysis

was performed in LS-Dyna software. The advantage of using the LS-Dyna software was that explicit solution methods were used instead of implicit analyses. Explicit analyses are usually more efficient and tend to be better equipped for highly transient and short duration simulations, which is the case for the simulations of this thesis [13].

Non-linear automatic surface-to-surface contact formulation was used since the shoe sample material is non-linear. The initial value of coefficient of friction was input as zero in order to isolate hysteresis friction from adhesion friction (i.e., the friction forces would only come from hysteresis friction and not due to friction from the contact algorithm) [29]. Most contact algorithms, termed penalty-based methods, try to eliminate the overlap or penetration between surface nodes by first detecting the amount of penetration and then applying an opposite force to remove these penetrations. For simulations of this thesis, second type soft constraint formulation was used for determining the contact stiffness according to the recommendations of Tokura [45]. This soft formulation is recommended by LS-Dyna when modeling the contact of the surfaces that have sharp corners and differing material properties, therefore it is appropriate for the rough geometries used in this study. This type of penalty-based contact calculates the contact stiffness based on actual time step in order to increase the contact stiffness with decreasing time step size and avoid element distortions. During model development, this contact algorithm was the only method capable of handling the large deformations of the soft rubber material and avoiding 'hourglassing' and 'checkerboarding' problems. In this method, initial penetrations are not eliminated but are instead used as the baseline from which additional penetration is measured [59], which are then used to calculate contact

forces. Lastly, the shoe sample was considered the slave material since it is softer and the floor sample was considered the master since it is harder.

2.5. Quantifying Coefficient of Friction for Hysteresis and Adhesion

Hysteresis coefficient of friction ($COF_{Hysteresis}$) was calculated by dividing average shear force by the average normal force between the two surfaces throughout the simulation by using Equation 9.

$$COF_{Hysteresis} = \frac{Average\ ShearForce}{Average\ NormalForce} \quad \ldots (9)$$

Adhesion frictional force is known to be approximately relative to the real area of contact [27] (Equation 10). Adhesion coefficient of friction ($COF_{Adhesion}$) is the ratio of adhesion friction force and the normal force for rubber [60] (Equation 11). Combining Equations 10 and 11 results in Equation 12, which can be used for quantifying the adhesion coefficient of friction. Hysteresis and adhesion coefficient of friction were calculated from model outputs that included shear force, normal force and contact area. An example plot of the output of the simulation (i.e. the variation of shear force, normal force and real area of contact) is shown in Figure. 10, Figure. 11 and Figure. 12 respectively.

$$F_{Adhesion} \propto Real\ area\ of\ contact \quad \ldots (10)$$

$$COF_{Adhesion} = \frac{F_{Adhesion}}{F_{Normal}} \quad \ldots (11)$$

$$COF_{Adhesion} \propto \frac{Real\ area\ of\ contact}{F_{Normal}} \quad \ldots (12)$$

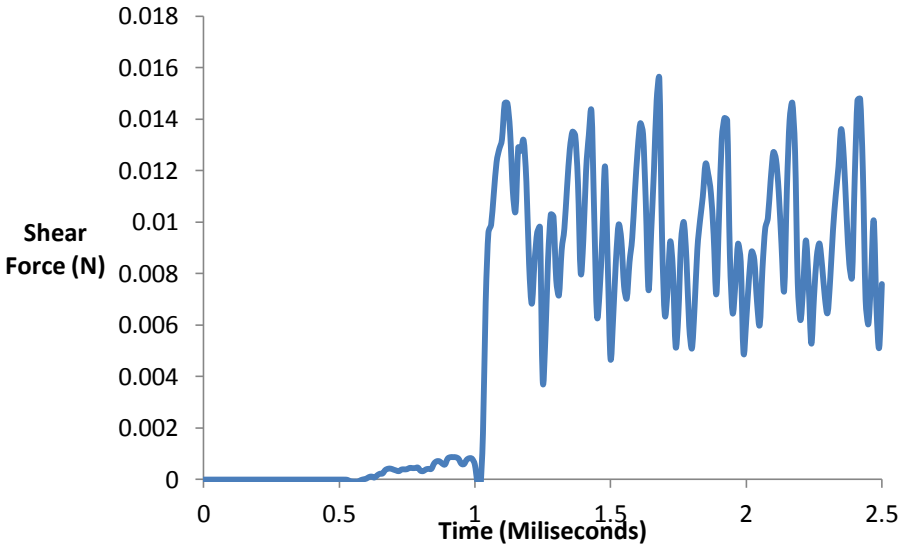

Figure 10. Shear force generated between shoe sample and floor sample model with respect to time (Rubber material. High floor roughness. High shoe roughness. Low force level)

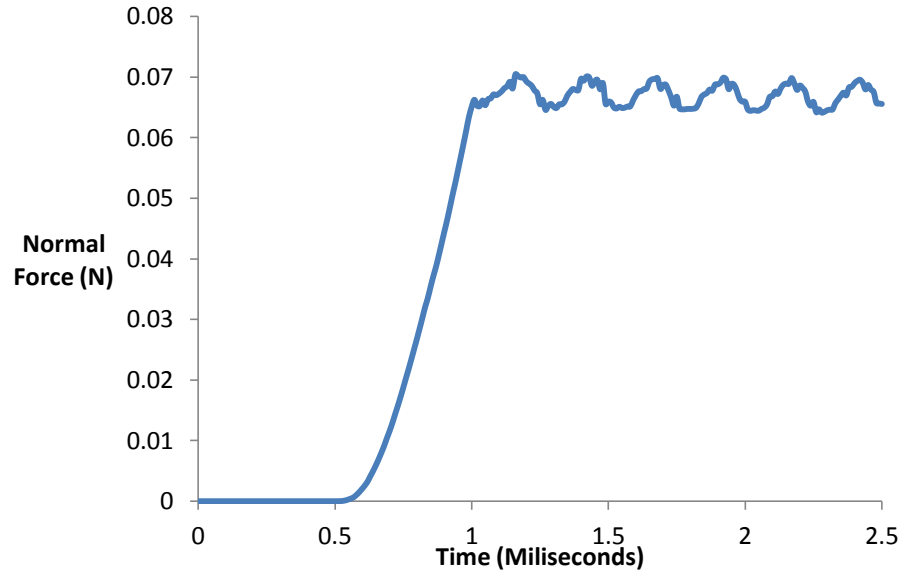

Figure 11. Normal force generated between shoe sample and floor sample model with respect to time (Rubber material. High floor roughness. High shoe roughness. Low force level)

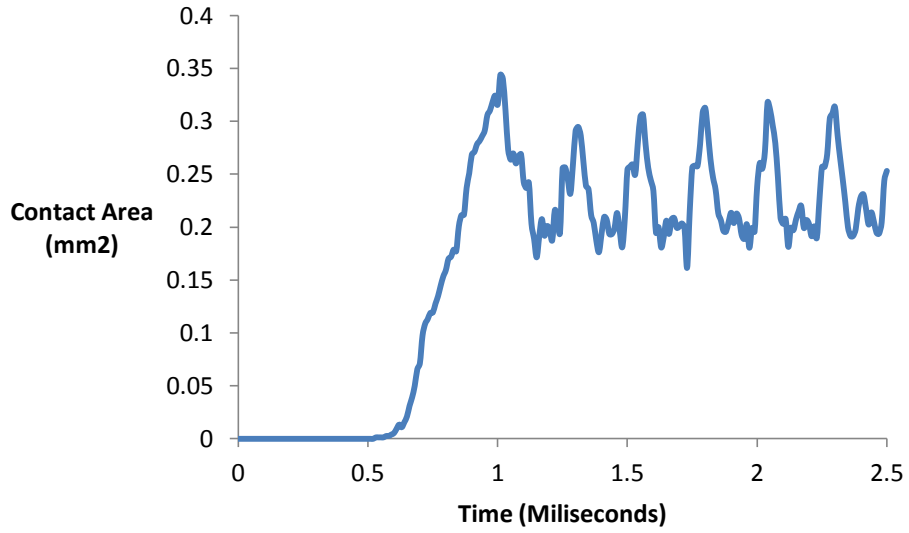

Figure 12. Real contact area between shoe sample and floor sample model with respect to time (Rubber material. High floor roughness. High shoe roughness. Low force level)

In order to determine the effects of sliding speed, simulations were performed in five different horizontal shoe speeds. Two different shoe roughness levels and three different levels of floor roughness were modeled to investigate the effect of shoe and floor roughness (Table 1). The two shoe materials used in this study were neolite and rubber (Table 3) to examine the effect of material properties. Also, the normal pressure was investigated by performing all simulations at three different contact pressure levels. Combinations of different levels of shoe sliding speed, shoe roughness, floor roughness, shoe material hardness and loading levels led to a total number of 180 simulations and the summary of their effects on adhesion and hysteresis is discussed in the next chapter.

3. Results and Discussion

3.1. Adhesion

The model indicated that sliding speed had a strong effect on real contact area, indicating that the adhesion friction is highly dependent on sliding speed. With increasing sliding speed from 0.1 m/s to 1 m/s, a decrease in ratio of real contact area to normal force was observed in both materials at all shoe and floor roughness levels (Figure 13A and 13B.). Neolite simulations showed a 16-29% decrease in ratio of real area of contact to normal force with increasing sliding speed from 0.1 to 1 m/s for different combinations of shoe-floor roughnesses while rubber simulations had a 12-25% decrease in adhesion friction with increasing sliding speed for different models with different shoe-floor roughness levels. These results that show a decreasing trend in real contact area and subsequently adhesion friction with increasing sliding speed are in close agreement with other research on polymers [61] and plastics [62] that discuss the effects of sliding speed on adhesion friction. As speed increases, the asperities spend less time in contact, which prevents the soft material from deforming around the asperities of the harder material and reduces the real contact area [25,63]. The recent experimental study of our group also supports the decrease in adhesion friction for shoe and floor materials with increasing speed in the range of 0-1 m/s [50].

A)

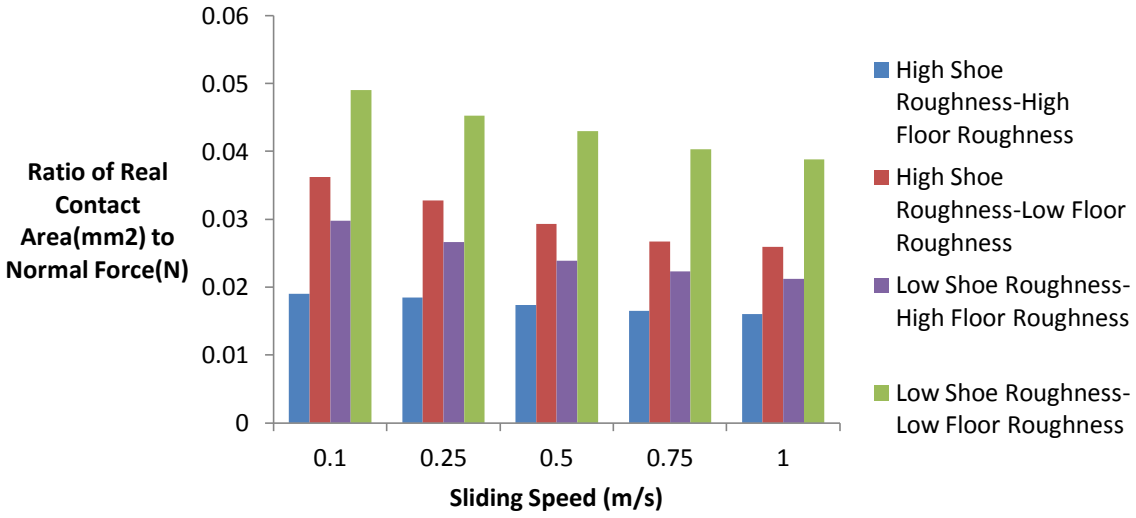

B)

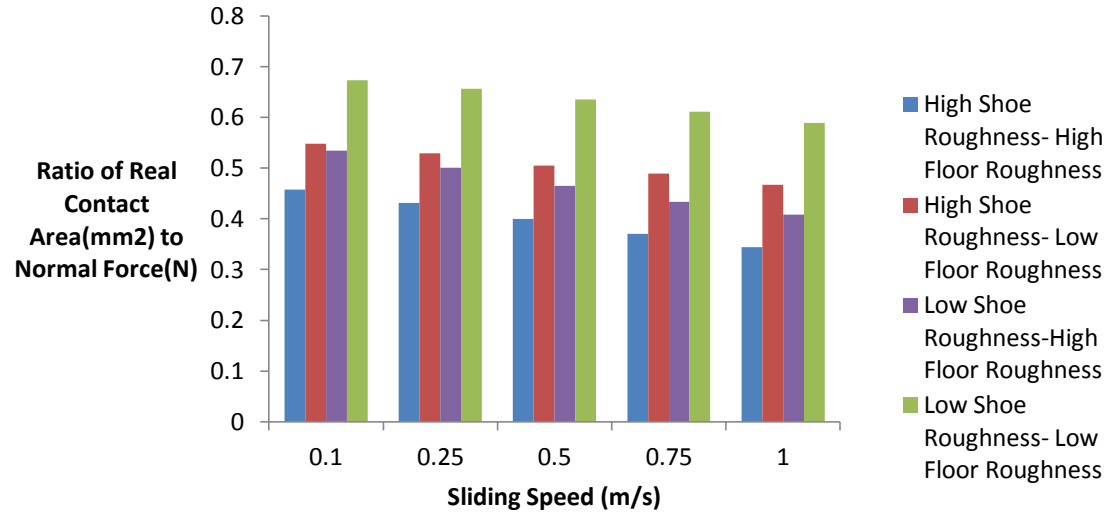

Figure 13. Variation of ratio of real contact area to normal force of neolite (A) and rubber (B) sample for different speeds for three combinations of shoe-floor roughness (Table 1.)

A negative correlation was observed between the shoe/floor roughness and the measure of adhesion friction (Figure 14A and 14B.). A 26-36% reduction in ratio of real area of contact to normal load was observed with increasing neolite shoe roughness in different floor roughness levels while increasing rubber shoe roughness caused a 14-18%

decrease in ratio of real area of contact to normal force for different floor roughnesses. Increasing floor roughness caused a 39-47% reduction in ratio of real area of contact to normal load in the neolite material while 17-21% decrease in adhesion was observed in rubber with increasing floor roughness. Therefore, adhesion was particularly dependent on shoe and floor roughness for the harder shoe material compared to the softer shoe material. The decrease in the ratio of real contact area to normal force with increasing shoe/floor roughness suggests that as asperity height is increased, the rigid floor asperities are not able to penetrate into the soft shoe material surface. This effect is consistent with tribological theory [30,64]. Experimental results on the effects of floor roughness on shoe-floor adhesion also show a reduction in adhesion friction with increasing floor roughness [65], [50]. Therefore, changing the shoe/floor roughness is a key parameter affecting the adhesion friction, especially for hard shoe materials.

A)

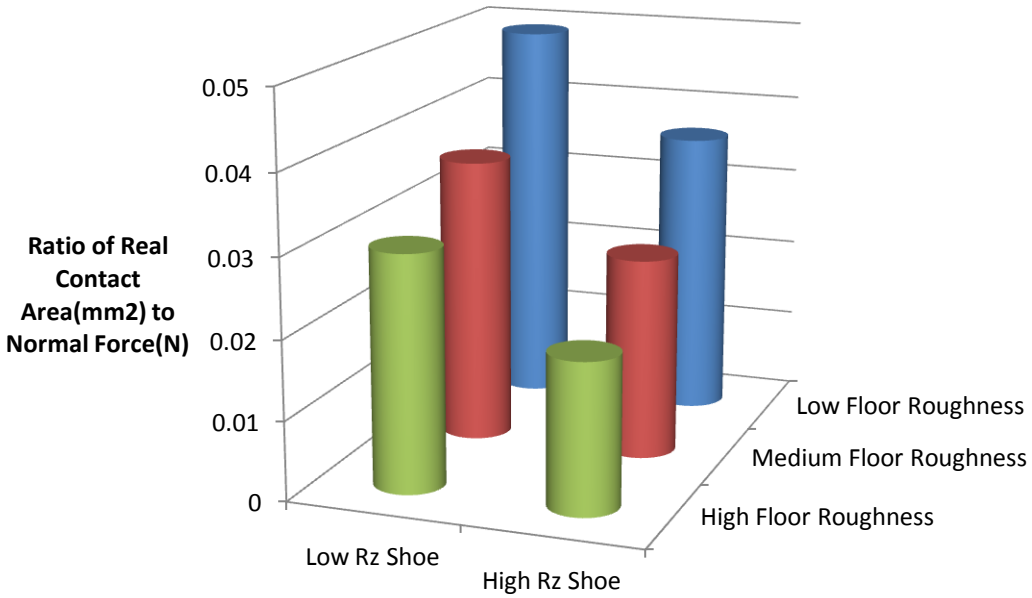

B)

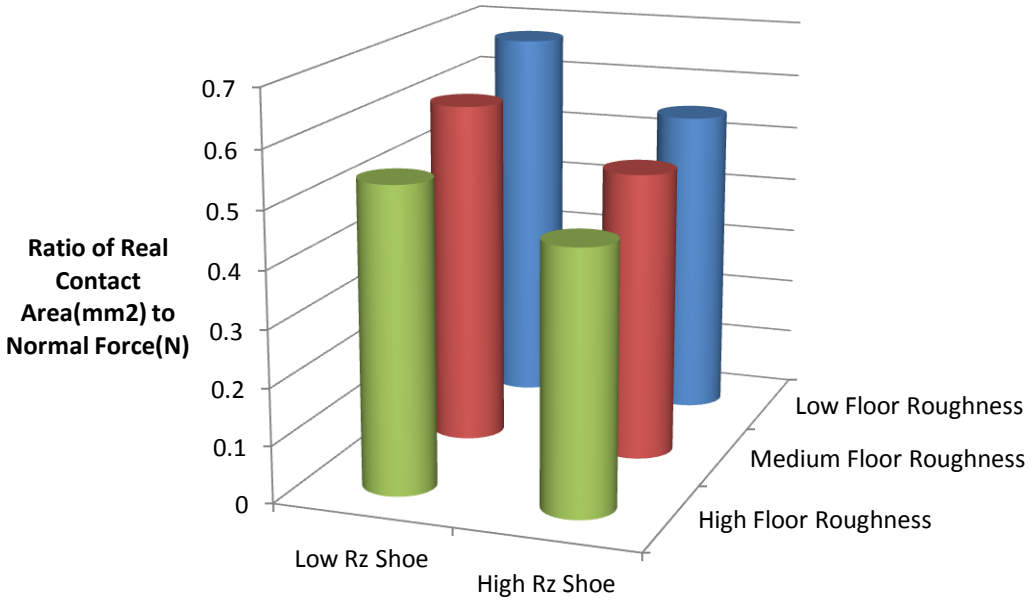

Figure 14. Variation of ratio of real contact area to normal force across different shoe/floor roughness (Table 1.) 0.1 m/s speed for neolite (A) and rubber (B) material.

The material properties had a substantial effect on the adhesion friction. Specifically, neolite had a more rigid long term and short term shear modulus than rubber (Table 3.), which influenced the adhesion results. Figure 15 shows that when the material hardness is increased, the ratio of the real area of contact to normal force is decreased by approximately 93-96% for different combinations of shoe-floor roughness. This result is supported by Bhushan who suggested that an increase in the modulus of elasticity decreases the real area of contact [30]. In general, soft and compliant materials are associated with higher adhesion due to an increase in the contact area between materials. This result shows that material hardness is a critical factor affecting the ratio of real contact area and normal force and thus it affects the adhesion friction [22, 66]. One important note, however, is that a change in contact area due to a change in material may not actually lead to a reduction in adhesion friction since the materials also influence the adhesion shear strength at the interface [60].

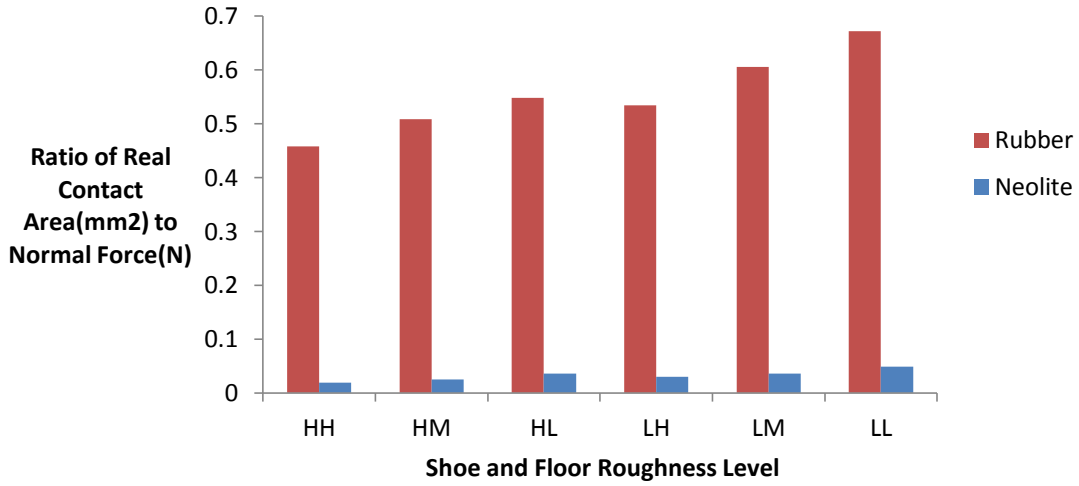

Figure 15. Variation of ratio of real area of contact and normal force for two different material properties (Table 3) in different combinations of shoe-floor roughness (Table 1) for 0.1 m/s speed. The first letter below each bar represents the shoe roughness level (H: high; L: low) and the second letter represents the floor roughness level (H: high; M: medium; L: low).

A negative correlation between normal loading i.e. contact pressure and ratio of real contact (proportional to adhesion friction) was observed (Figure 16). Increasing normal load from 160 kPa to 360 kPa led to a 4% and 27% decrease in ratio of real area of contact to normal load for neolite and rubber respectively. This finding is supported by the pioneering work of Schallamach [67] and Bhushan [30] who suggested that in rubber friction, adhesion coefficient of friction is proportional to the inverse of cube root of normal load meaning that increasing normal load will lead to decreasing adhesion coefficient of friction. Moreover, a recent study using pin-on-disk tribometer has examined the effect of varying normal load on adhesion friction in elastomers and concluded that an increased normal pressure will result in decreased adhesion [68] due to saturation in contact area. Since normal load is in the denominator in equation for adhesion coefficient of friction (Equation 12.), a constant contact area and increasing normal load will lead to a decrease in adhesion COF with increasing normal load. This

concept can be applied to the models developed in this thesis for the soft rubber material. This effect is more significant in soft material as it is also clear from Figure 16.

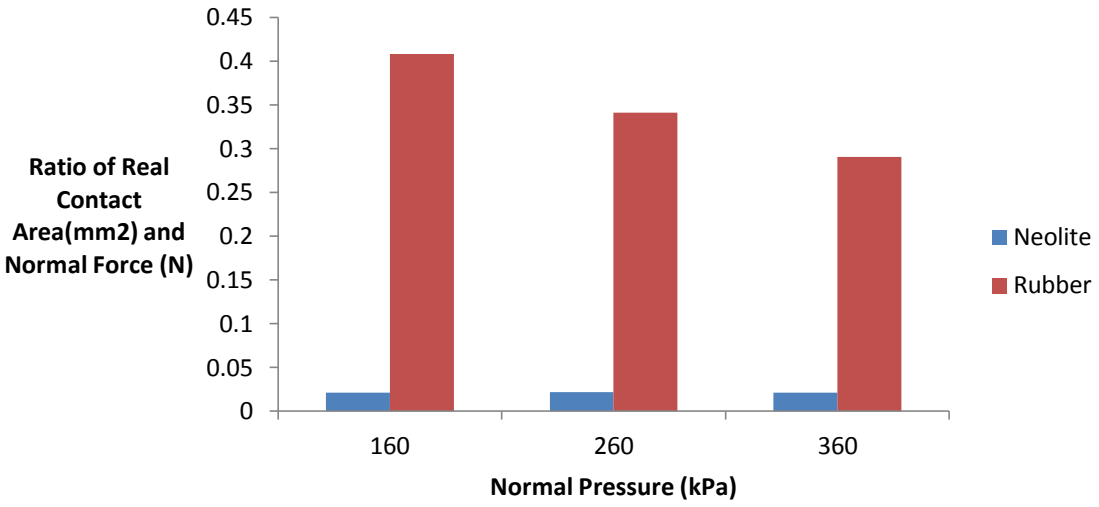

Figure 16. Variation of ratio of real contact area to normal force for two different material properties (Table 3). Low shoe roughness and high floor roughness for 1m/s speed.

3.2. Hysteresis

Hysteresis friction responded inconsistently to increases in sliding speed dependent on the shoe material and shoe/floor roughness levels. (Figure. 17A and 17B). The majority of shoe/floor combinations showed an increase in hysteresis friction with sliding speed although the high roughness neolite demonstrated a negative trend when sliding against low roughness flooring. Studies on effects of sliding speed on friction show that for low speeds, hysteresis friction increases, but for higher speeds friction decreases or remain constant [61, 69-71]. Results of previous finite element modeling of shoe and floor materials [29] also reported a constant trend for hysteresis friction with increasing speed, which supports most of the results of the thesis' simulations. Experimental results from Beschorner report a decrease in overall friction [21] and

hysteresis coefficient of friction [50] when increasing sliding speed, due to increases in hydrodynamic pressures within a fluid contaminant [72]. Decreases in friction due to hydrodynamic effects likely counteract the increase in hysteresis friction. The models presented in this thesis did not include the fluid contaminant component and therefore are not able to capture the effects of fluid pressure. Thus, the inconsistencies between these trends in hysteresis and experimental data necessitate the need for a hybrid model that includes the effects of both fluid and solid fields to be able to more accurately predict the effect of sliding speed on hysteresis friction similar to the model developed in [20].

A)

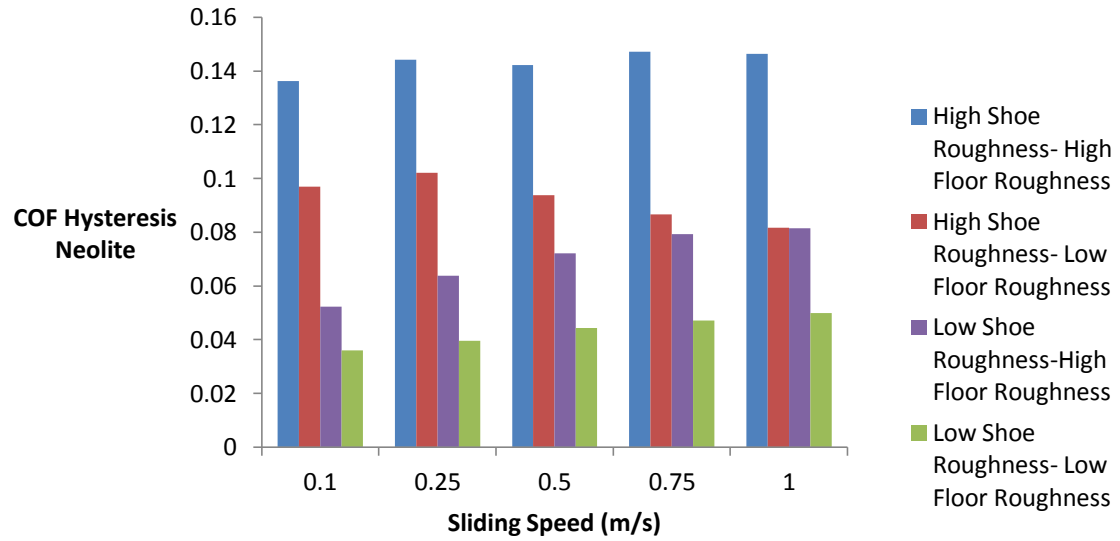

B)

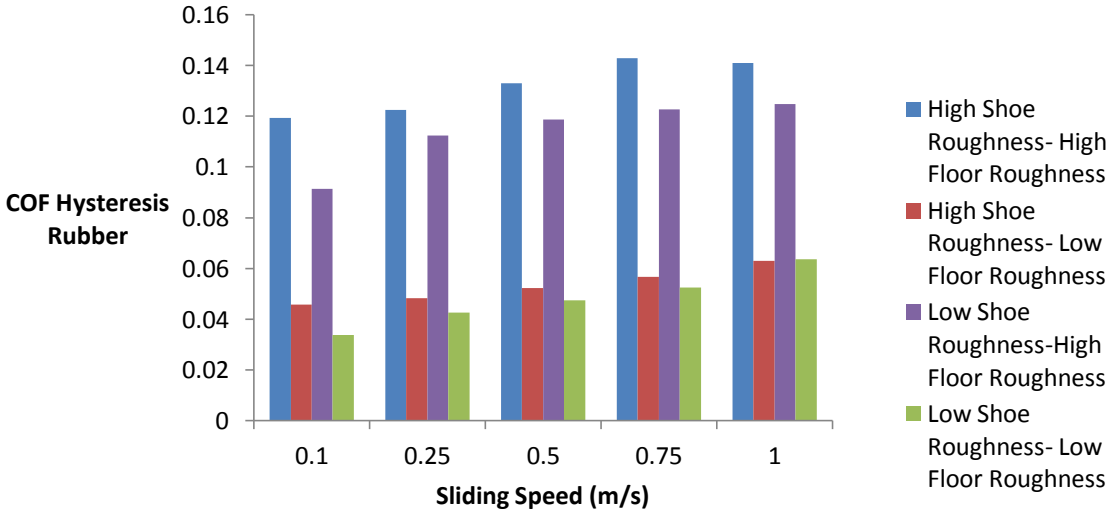

Figure 17. Variation of hysteresis coefficient of friction of neolite (A) and rubber (B) sample for different speeds for three combinations of shoe-floor roughness (Table 1.)

A positive correlation between asperity height of either the shoe or floor material and $COF_{Hysteresis}$ was identified for both of the materials (Figure. 18A and 18B). A 161-169% increase in hysteresis coefficient of friction was observed with increasing neolite shoe roughness, while increasing rubber shoe roughness caused a 10-35% increase in

hysteresis coefficient of friction. Increasing floor roughness caused a 42-45% increase in hysteresis coefficient of friction in the neolite material while a 164-170% increase in hysteresis coefficient of friction was observed in rubber. This increased hysteresis with increased roughness tends to be more significant in the neolite shoe material when changing shoe roughness and more significant in rubber material when changing floor roughness. The increase in hysteresis friction is due to the development of high stress in the shoe sample model due to a harder material or greater roughness as shown in Figure 19. The larger asperities of the rougher materials result in larger deformation in the shoe sample. The shoe sample follows a viscoelastic material model, so the energy loss due to these deformations and stresses is not completely restored [46]. Thus, some portions of this energy is lost and contributes to an increase in friction through hysteresis mechanism [40,73,74]. Since the neolite is harder, higher stresses will be developed and therefore roughness will have a larger effect on its hysteresis coefficient of friction (Figures 18A and 18B). These results are in close agreement with the experimental results of Cowap and Beschorner who reported an increase in hysteresis friction with increasing floor roughness [50,65]. Previous finite element simulations dealing with rubber friction also reported a positive correlation between hysteresis friction and roughness [75]. Therefore, roughness is an important factor that affects the hysteresis friction in shoe-floor friction complex.

A)

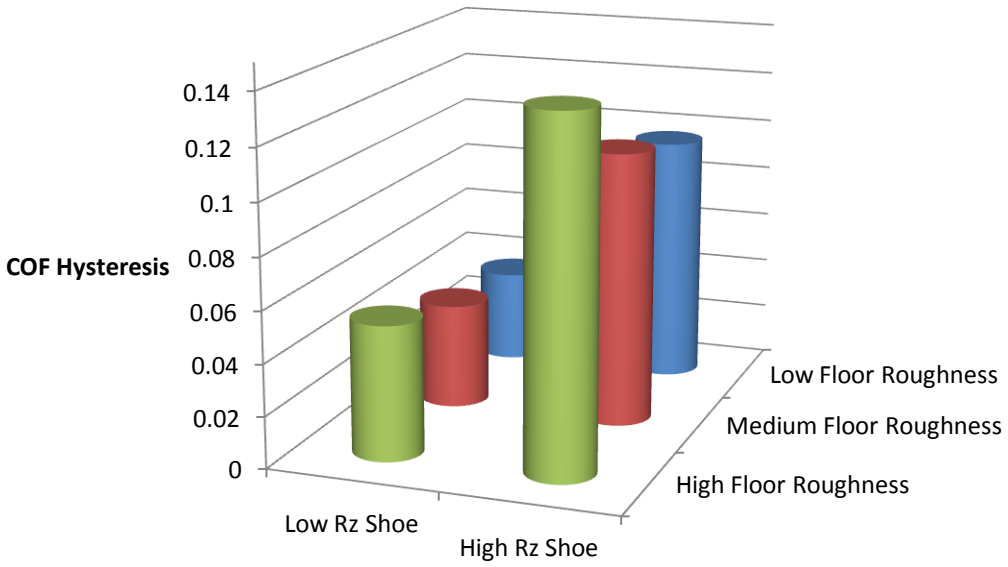

B)

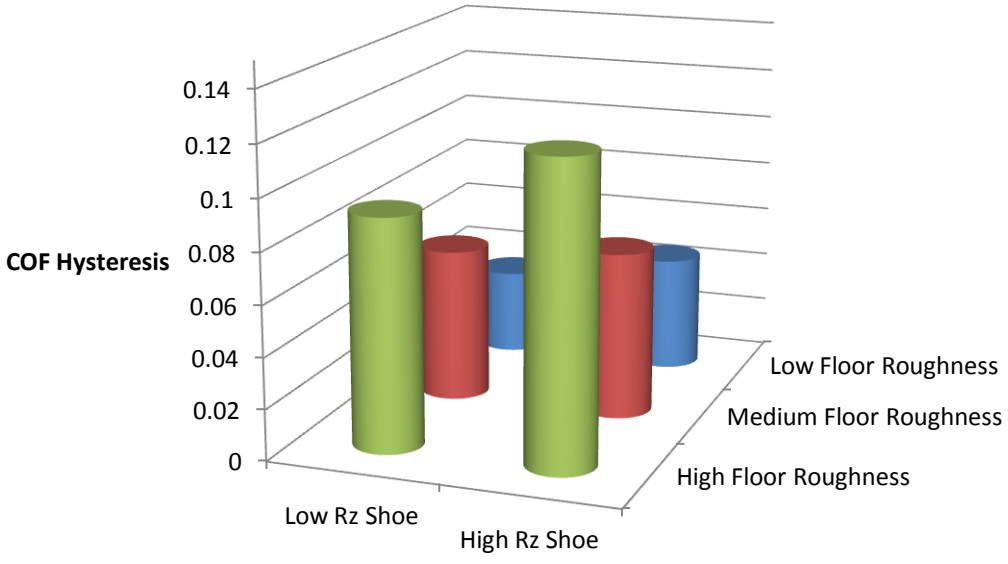

Figure 18. Variation of $COF_{Hysteresis}$ with shoe/floor roughness (Table 1.) for 0.1 m/s speed with neolite (A) and rubber(B) material.

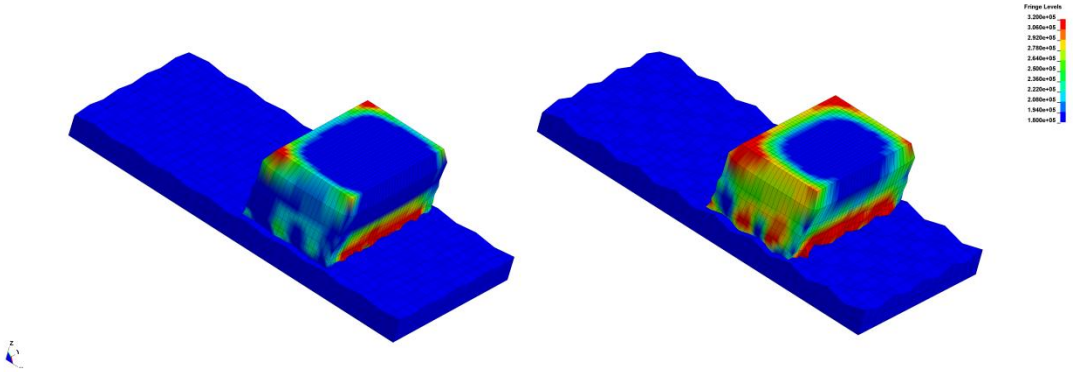

Figure 19. Higher von mises stress developed during sliding of high shoe roughness on high floor roughness (Right) compared to low shoe roughness-low floor roughness combination (Left). Rubber material in 1m/s sliding speed.

As a demonstration of the value of this model, the model was implemented to determine why hysteresis friction is higher for a high roughness rubber material compared with a low roughness neolite material as it is reported here and in [50]. The neolite material has a higher hysteresis coefficient of friction at high shoe roughness, yet the neolite hysteresis friction is substantially reduced in the low roughness condition (approximately by 62%). In order to achieve a certain level of contact pressure, the softer material needs to be pushed more towards the rigid floor and it will have more interaction with the flooring. Because the softer shoe material conforms to the topography of the flooring, the roughness of the shoe material is less important than the roughness of the hard shoe material. Since neolite is harder, it will develop higher stresses although these stresses will only contribute to hysteresis friction when the slope of the asperities is great enough to cause the stress to be occurring laterally as opposed to vertically. Thus, an important interaction between the material properties and the material topography exists (Figure 20). Therefore, the greater hysteresis friction that was observed within this study

and in [50], is not solely due to differences in the material properties but also because the soft rubber material had a rougher surface than the neolite. Therefore, selecting shoe materials that stay rough even as they experience wear may be an attractive strategy for preventing slipping accidents, particularly if a hard shoe material is used.

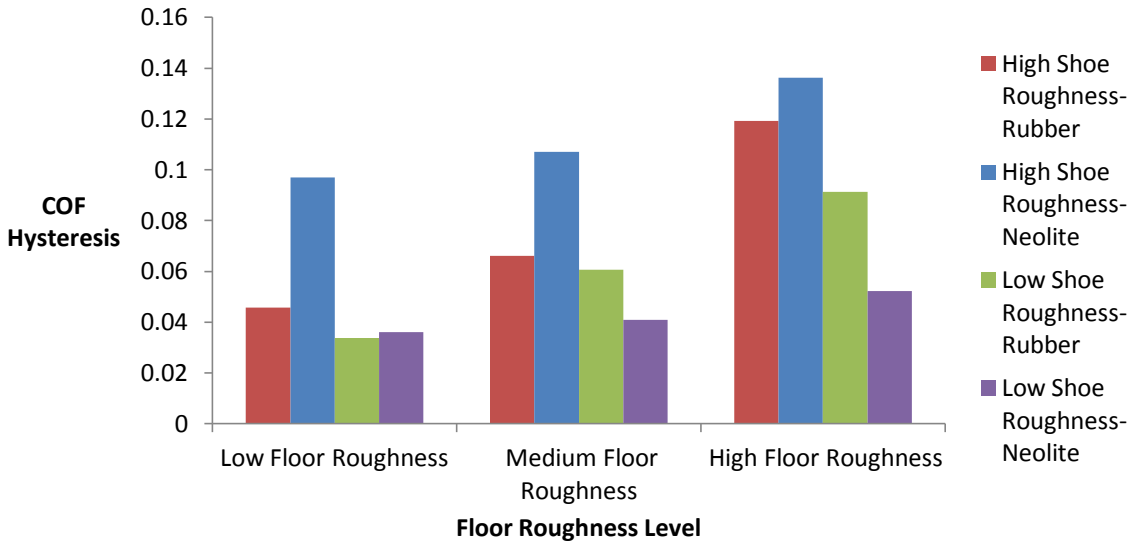

Figure 20. Variation of $COF_{Hysteresis}$ for the two different material properties (Table 3) with different shoe/floor roughness combinations. Sliding speed of 0.1 m/s

An illustration of the von mises stress distribution for the shoe model during sliding motion is shown in Figure 21. The figure shows the contours where the von mises stress is developed in the rubber material model. It can be seen that the high stress areas are in the vicinity of the interacting asperities. These stresses in the shoe material contribute to the energy dissipation in the form of hysteresis friction in the viscoelastic shoe material.

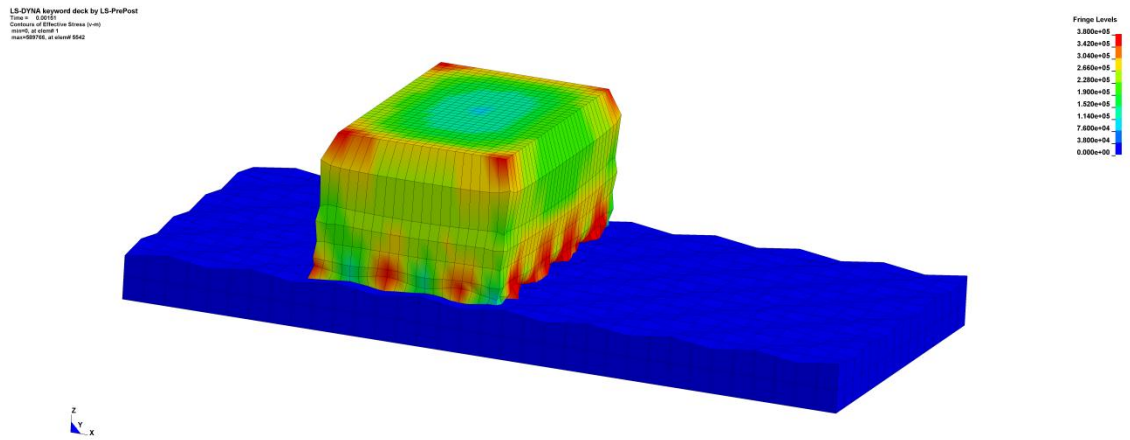

Figure 21. Von mises stress during the sliding motion of rubber shoe sample model over the rigid floor.

With increasing the normal load, a decreasing trend in hysteresis coefficient of friction was observed as it is shown in Figure 22. Increasing normal load from 160 kPa to 360 kPa led to a 9% and 25% decrease in hysteresis coefficient of friction for neolite and rubber respectively. This finding is in agreement with a relatively new experimental study about footwear friction [76] that suggests that in shoe-floor friction, horizontal force does not increase as quickly as normal force, causing a decreased contribution to the total hysteresis friction with increasing normal load. This phenomenon is also reported by Bhushan [30].

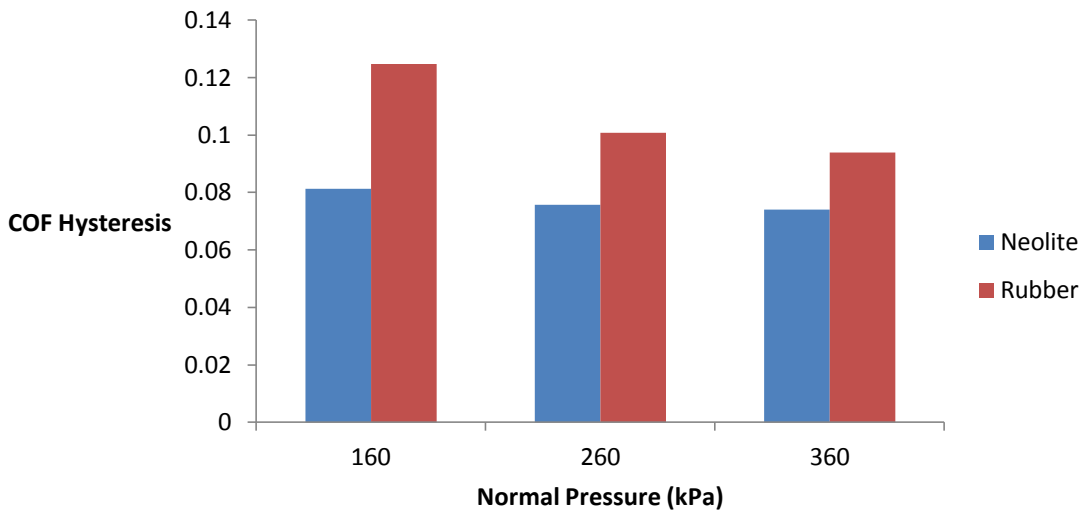

Figure 22. Variation of hysteresis coefficient of friction for the two different material properties (Table 3). Low shoe roughness and high floor roughness for 1m/s speed.

4.Conclusion

In this thesis, development of the three dimensional shoe and floor microscopic model confirms that shoe and floor roughness, shoe sole sliding speed, shoe material properties and normal loading affect the adhesion and hysteresis component of shoe-floor friction in dry and boundary lubrication regimes. According to the findings of this thesis, roughness can be considered as the primary factor that affects the adhesion and hysteresis friction. The increase in roughness, increases hysteresis friction and decreases the ratio of real area of contact and normal force (proportional to adhesion friction). Secondly, increase in the sliding speed of the shoe sample model decreases the ratio of real area of contact to normal force (adhesion friction) and has inconsistent effects on hysteresis friction. Shoe material properties played an important role in changing adhesion friction with softer shoe material having a significantly higher adhesion friction. Normal loading had also a slight effect on adhesion and hysteresis components with increasing normal load leading to a reduction in both components. The model generated responses to roughness, material properties and boundary conditions that are generally consistent with tribological theory and experimental data. The one notable exception was the positive correlation between hysteresis friction and sliding speed, which is opposite to the trends observed in experimental studies. This discrepancy can be explained given that hydrodynamic effects, which were not included in this model, become increasingly more important at higher sliding speeds.

These findings from the computer simulations of viscoelastic shoe material and the rigid floorings suggests that shoe and floor roughness, sliding speed and material properties are the most important parameters for understanding the hysteresis and

adhesion friction in shoe-floor slip events and controlling these parameters can be useful in designing slip-resistant shoe and flooring surfaces. According to findings of this thesis, in order to increase hysteresis, which is more relevant to oily surfaces, increasing shoe/floor roughness is an effective way. However, shoe/floor roughness has the opposite of this effect on adhesion, which is more relevant to dry/wet surfaces. Therefore, decreasing surface roughness would improve friction in this condition. Since adhesion and hysteresis had different trends with increasing shoe/floor roughness, finding an optimum roughness that enhances both hysteresis and adhesion friction would be valuable. According to the findings of this thesis on the effect of normal loading on friction, designing surfaces that distribute the normal load and lower the normal pressure will lead to an improvement in both adhesion and hysteresis friction. Having softer material for shoe will also help in increasing adhesion component.

This thesis identified roughness as an important factor in shoe-floor friction, however use of a two dimensional profilometer and creating three dimensional asperities and roughness according to that might not be representative of the actual surface roughness. There are also studies that report length scale effect in surface asperities as an important factor affecting rubber like material contacts. Roughness parameters calculated from 3D profilometry tend to be larger than when recorded with 2D profiles, indicating that using 3D profilometry would lead to larger hysteresis values and smaller contact area values. Therefore, future research should concentrate on different asperity shapes and profiles utilizing the surface profiles obtained from shoe and floor geometries using three dimensional profilometry techniques and three dimensional roughness parameters. To further investigate the effect of material properties on shoe-floor friction, more modeling

trials can performed with different viscoelastic materials having different bulk moduli, long time and short time shear moduli and decay constants to optimize these parameters for maximizing adhesion and hysteresis components. This study also considered static loading, which may have over-simplified the dynamic process of stepping. Future studies that include dynamic loading may find differences in material response and friction values. Moreover, in this thesis, a constant value for Poisson's ratio of the rubber was assumed based on the values reported in the literature. Measuring Poisson's ratio of the shoe samples and implementing it into modeling studies can also yield more reliable results. Using the results from the experimental studies, simulations can be validated and improved and the results of the simulations can help in defining improved experimental procedures for shoe-floor friction analysis. Therefore, the results of simulations and modeling studies can be used to complete each other and the set of experiments and simulations together will enhance the shoe-flooring design and increase the shoe-floor friction leading to a reduction in slip and fall accidents.

References

1. National Floor Safety Institute: Causes of Slips, Trips & Falls. 2012 .

http://www.nfsi.org/pdfs/Causes.pdf

2. Liberty Mutual Research Institute, 2012. Liberty Mutual Workplace Safety Index.

3.Environmental Health & Safety. 2013 . Slip, Trip and Fall Prevention. Carnegie Mellon University, Pittsburgh, PA, USA.

4. U.S. Department of Labor. Bureau of Labor Statistics, 2012 Census of Fatal Occupational Injuries Table 2. Fatal occupational injuries by industry and selected event or exposure, Washington, D.C.

5. U.S. Department of Labor. Bureau of Labor Statistics, 2012 Nonfatal Occupational Injuries and Illnesses Requiring Days Away From Work: Table 5. Number, incidence rate, and median days away from work for nonfatal occupational injuries and illnesses involving days away from work by selected injury or illness characteristics and private industry, state government, and local government, Washington, D.C.

6. Courtney, T K., Sorock, G. S., Manning, D. P., Collins, J. W. & Holbein Jenny M. A., 2001. Occupational slip, trip, and fall related injuries. Can the contribution of slipperiness be isolated? Ergonomics, 44, 11, 18-1137.

7. Hanson, J.P., Redfern, M.S., Mazumdar, M .,1999. Predicting slips and falls considering required and available friction. Ergonomics 42, 12, 1619-1633.

8. Perkins, P.J., Measurement of slip between shoe and ground during walking. ASTM-Special-Technical_Publication, ASTM STP 649, 1978: p. 71-87.

9. Proctor, T.D. and V. Coleman, Slipping, tripping and falling accidents in Great Britain - Present and future. Journal of Occupational Accidents, 1988. 9(4): p. 269-285.

10. Strandberg, L., On accident analysis and slip-resistance measurement. Ergonomics, 1983. 26(1): p. 11-32.

11. Burnfield, J. & Powers, C., 2006. Prediction of slip events during walking: An analysis of utilized coefficient of friction and available slip resistance. Ergonomics, 49, 982-985.

12. Marpet, M., On threshold values that separate pedestrian walkways that are slip resistant from those that are not. Journal of Forensic Sciences, 1996. 41(5): p. 747-755.

13. Beschorner. K.E. Development of a computational model for shoe-floor-contaminant friction, PhD Thesis 2008, University of Pittsburgh, Pittsburgh, Pa.

14. Grönqvist, R. Mechanisms of friction and assessment of slip resistance of new and used footwear soles on contaminated floors. Ergonomics 38(2), 224-241 (1995).

15. Li, K. W. & Chen, C. J., 2004. The effect of shoe soling tread groove width on the coefficient of friction with different sole materials, floors, and contaminants. Applied Ergonomics, 35, 499-507

16. Li, K. W., Wu, H. H. & Lin, Y. C., 2006. The effect of shoe sole tread groove depth on the friction coefficient with different tread groove widths, floors and contaminants. Applied Ergonomics, 37, 743-748.

17. Strobel, C.M., Menezes, P., Lovell, M., Beschorner, K.E. (2012). Analysis of the contribution of adhesion and hysteresis to shoe-floor lubricated friction in the boundary lubrication regime, Tribology Letters, 47:3, 341-347.

18. Redfern, M.S. and B. Bidanda, Slip resistance of the shoe-floor interface under biomechanically-relevant conditions. Ergonomics, 1994. 37(3): p. 511-524.

19. Moore, C.T., Menezes, P.L., Lovell, M., Beschorner, K.: Analysis of shoe friction during sliding against floor material: Role of fluid contaminant. Journal of Tribology 134, 041104 (2012).

20. Beschorner, K., Lovell, M., Higgs III, C.F., Redfern, M.S.: Modeling mixed-lubrication of a shoe-floor interface applied to a Pin-on-Disk apparatus. Tribology Transactions 52(4), 560-568 (2009).

21. Beschorner, K.E., M.S. Redfern, W.L. Porter, and R.E. Debski, Effects of slip testing parameters on measured coefficient of friction. Applied Ergonomics, 2007. 38(773-780).

22. Chang, W.-R. and S. Matz, The slip resistance of common footwear materials measured with two slipmeters. Applied Ergonomics, 2001. 32(6): p. 549-558.

23. Chang, W.R., In-Ju Kim, Derek P. Manning, and Yuthachai Bunterngchit, The role of surface roughness in the measurement of slipperiness. Ergonomics, 2001. 44(13): p. 1200-1216.

24. Chang, W.-R., Grönqvist, R., Hirvonen, M., Matz, S.: The effect of surface waviness on friction between neolite and quarry tiles. Ergonomics 47(8), 890-906 (2004)

25. Chang, W.-R., et al., The role of friction in the measurement of slipperiness, Part 1: Friction mechanisms and definition of test conditions. Ergonomics, 2001. 44(13): p. 1217-1232.

26. Moore, The friction of pneumatic tyres,1975, Amsterdam: Elsevier.

27. Tabor. Friction, adhesion and boundary lubrication of polymers, in L.-H. Lee (ed.). Advances in Polymer Friction and Wear, Polymer Science and Technology. Vol. 5A. 1974, New York: Plenum Press.

28. Strandberg, L., The effect of conditions underfoot on falling and overexertion accidents. Ergonomics, 1985. 28: p. 131-147.

29. Singh, G.: Analysis of shoe-floor slipperiness through computational modeling and measurements of hydrodynamic pressures with robotic slip simulator. University of Wisconsin - Milwaukee (2012)

30. Bhushan, B., Introduction to Tribology2002, New York: John Wiley & Sons.

31. Singh, G. & Beschorner, K., 2013. A method for measuring hydrodynamic lubrication in the shoe floor fluid Interface: Application to shoe tread evaluation. Ergonomics, in review.

32. Brodsky, J.W., et al., Objective evaluation of insert material for diabetic and athletic footwear. Foot Ankle, 1988. 9(3): p. 111-6.

33. Edwards, J. and K. Rome, A study of the shock attenuating properties of materials used in chiropody. The Foot, 1992. 2(2): p. 99-105.

34. Jason Tak-Man Cheung, Jia Yua, Duo Wai-Chi Wonga & Ming Zhanga. Current methods in computer-aided engineering for footwear design. Footwear Science 1(1). 2009 pp 31-46

35. Lewis, G.: Finite element analysis of a model of a therapeutic shoe: effect of material selection for the outsole. Biomed. Mater. Eng. 13(1), 75–81 (2003)

36. Sun, Z., D. Howard, and M. Moatamedi, Finite-element analysis of footwear and ground interaction. Strain, 2005. 41(3): p. 113-115.

37. McFarlane, J.S. and D. Tabor, Adhesion of solids and the effect of surface films. Proceedings of the Royal Society of London. Series A. Mathematical and Physical Sciences, 1950. 202(1069): p. 224-243.

38. Moore, A.C.a.T., D., Some mechanical and adhesive properties of indium. British Journal of Applied Physics, 1952. 3: p. 299-301.

39. Adhesion model for metallic rough surfaces. Trans. ASME, J. Tribol., 1988. 110(1): p. 50.

40. Persson, B.N.J., Theory of rubber friction and contact mechanics. The Journal of Chemical Physics, 2001. 115(8): p. 3840-3861.

41. L.A. Gracia, E. Liarte, J.L. Pelegay, B. Calvo, Finite element simulation of the hysteretic behaviour of an industrial rubber. Application to design of rubber components

.Finite Elements in Analysis and Design. 46,(4), 2010, Pp 357‑368

42. F.J. Martínez, M. Canales, S. Izquierdo, M.A. Jiménez, M.A. Martínez, Finite element implementation and validation of wear modelling in sliding polymer‐metal contacts. 284‐285 (25) ,2012, Pp 52‐64

43. J.M. Bielsa, M. Canales, F.J. Martínez, M.A. Jiménez, Application of finite element simulations for data reduction of experimental friction tests on rubber–metal contacts, Tribology International, 43 (4), 2010, Pp 785-795

44. P. Gabriel, A.G. Thomas, J.J.C. Busfield, Influence of interface geometry on rubber friction, Wear, Volume 268, 5–6, 11, 2010, Pp 747-750

45. Tokura. S. Contact and sliding simulation of rubber disk on rigid surface with microscopic roughness.6th European LS-DYNA Users' Conference , 2007

46. Bui, Q.V. and J.P. Ponthot, Estimation of rubber sliding friction from asperity interaction modeling. Wear, 2002. 252(1–2): p. 150-160.

47. Bryson, J.A., Impact response of polyurethane, 2009. Master's Thesis, Department of Mechanical Engineering,. Washington State University.

48. Chang, W.-R.: The effect of surface roughness on dynamic friction between neolite and quarry tile. Safety Science 29(2), 89-105 (1998).

49. Chang, W.-R., Hirvonen, M., Grönqvist, R.: The effects of cut-off length on surface roughness parameters and their correlation with transition friction. Safety science 42(8), 755-769 (2004).

50. M. J. H. Cowap, S. R. Moghaddam, P. L. Menezes & K. E. Beschorner. Contributions of adhesion and hysteresis to the coefficient of friction between shoe and floor surfaces: Effects of floor roughness and sliding speed, 2013. Submitted to Tribology Letters.

51. Erhart, T., Review of solid element formulations in LS-DYNA: Properties, limits, advantages, disadvantages", 2011 Developers' Forum, Stuttgart, Germany, October, 2011.

52. Hermann, L., R. and F.E. Peterson, A numerical procedure for viscoelastic stress analysis. Seventh Meeting of ICPRG Mechanical Behaviour Working Group, Orlando,FL, CPIA, 1968. Publication No. 177.

53. Densities of miscellaneous solids, 2013. http://www.engineeringtoolbox.com/density-solids-d_1265.html

54. J. Yura, A. Kumar, A. Yakut, C. Topkaya, E. Becker, & J. Ollingwood. National Cooperative Highway Research Program. CHRP Report 449. Elastomeric bridge bearings: Recommended test methods, 2001. Appendix B. Annex C

55. Suh, J. B., Stress analysis of rubber blocks under vertical loading and shear loading, Ph.D. Dissertation, Dept. of Mechanical Engineering, University of Akron, August, 2007.

56. Centeno G. O. Finite element modeling of rubber bushing for crash simulation. Experimental tests and validation. Master's Thesis. Division of Structural Mechanics, LTH, Lund University Sweden, September, 2009.

57. Y. C. Fung, A First course in continuum mechanics, Prentice-Hall, Englewood Cliffs, New Jersey, 1977

58. P.H. Mott, J.R. Dorgan, C.M. Roland, The bulk modulus and Poisson's ratio of "incompressible" materials, Journal of Sound and Vibration, Volume 312, Issues 4–5, 20 May 2008, Pages 572-575

59. Contact modeling in LS-Dyna and soft option - LS-DYNA Support - the LS-DYNA support site, http://www.dynasupport.com/howtos/contact/soft-option

60. Heinrich, G. and M. Klüppel, Rubber friction, tread deformation and tire traction. Wear, 2008. 265(7–8): p. 1052-1060.

61. Myshkin, N.K., M.I. Petrokovets, and A.V. Kovalev, Tribology of polymers: Adhesion, friction, wear, and mass-transfer. Tribology International, 2005. 38(11–12): p. 910-921.

62. W.C. Milz, L.E.S., Frictional characteristics of plastics. Lubrication Eng, 1955. 11: p. 313-317.

63. Yang, C., Persson, B.: Contact mechanics: contact area and interfacial separation from small contact to full contact. Journal of Physics: Condensed Matter 20(21), 215214 (2008).

64. Le Feng Wang, B.G., Gui Ming Huang, Wei Bin Rong, Li Ning Sun, Effects of asperity shape on the adhesion hysteresis originated from surface roughness. Advanced Materials Research 2011. 213: p. 201-205

65. Cowap., M., Beschorner., K., The effects of floor roughness on shoe-floor friction adhesion and hysteresis. International Joint Tribology Conference 2012.

66. Moore, D.F., The friction and lubrication of elastomers. International Series of Monographs on Material Science and Technology, ed. G.V. Raynor. Vol. 9. 1972: Oxford: Pergamon Press.

67. Schallamach A. The load dependence of rubber friction 1952 Proceedings of the Physical Society. 65 (9)

68. Farroni. F, Russo. M, Russo. R. & Timpone. F. Tyre-road interaction: Experimental investigations about the friction coefficient dependence on contact pressure, road roughness, slide velocity and temperature (2012) ASME Proceedings in Advanced Materials and Tribology, Nantes, France.

69. Flom, D.G. and N.T. Porile, Effects of temperature and high-speed sliding on the friction of Teflon on Teflon. Nature, 1955. 175(4459): p. 682-682.

70. Flom, D.G. and N.T. Porile, Friction of Teflon sliding on Teflon. Journal of Applied Physics, 1955. 26(9): p. 1088-1092.

71. Fort, T., Adsorption and boundary friction on polymer surfaces. The Journal of Physical Chemistry, 1962. 66(6): p. 1136-1143.

72. Beschorner. K, Albert. D, Chambers. A, Redfern .M , Fluid pressures at the shoe–floor–contaminant interface during slips: Effects of tread & implications on slip severity, Journal of Biomechanics, Available online 7 November 2013, ISSN 0021-9290, http://dx.doi.org/10.1016/j.jbiomech.2013.10.046.

73. Grosch, K.: The relation between the friction and visco-elastic properties of rubber. Proceedings of the Royal Society of London. Series A. Mathematical and Physical Sciences 274(1356), 21-39 (1963).

74. Heinrich, G.: Hysteresis friction of sliding rubbers on rough and fractal surfaces. Rubber chemistry and technology 70(1), 1-14 (1997).

75. László Pálfi, N.B., Tibor Goda, Károly Váradi, Árpád Czifra, FE simulation of the hysteretic friction considering the surface topography. Per. Pol. Mech. Eng, 2008.

76. Adam. C, Piotrowski. Use of the unified theory of rubber friction for slip-resistance analysis in the testing of footwear outsoles and outsole compounds (2012) .Footwear Science, 4(1), Pp 23-35